

# Accessibilome of Human Glioblastoma: Collagen-VI-alpha-1 Is a New Target and a Marker of Poor Outcome

Andrei Turtoi,<sup>\*,†,§,#</sup> Arnaud Blomme,<sup>†,#</sup> Elettra Bianchi,<sup>‡</sup> Pamela Maris,<sup>†</sup> Riccardo Vannozzi,<sup>||</sup> Antonio Giuseppe Naccarato,<sup>⊥</sup> Philippe Delvenne,<sup>‡</sup> Edwin De Pauw,<sup>§</sup> Generoso Bevilacqua,<sup>⊥</sup> and Vincent Castronovo<sup>†</sup>

<sup>†</sup>Metastasis Research Laboratory, GIGA-Cancer and <sup>‡</sup>Department of Pathology, University of Liege, Bat. B23, Liege 4000, Belgium

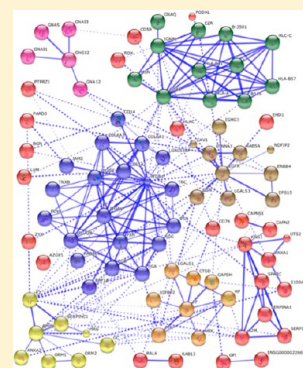
<sup>§</sup>Laboratory of Mass Spectrometry, GIGA-Research, University of Liege, Bat. B6, Liege 4000, Belgium

<sup>||</sup>Department of Neurosurgery, <sup>⊥</sup>Division of Surgical, Molecular and Ultrastructural Pathology, Pisa University Hospital, Pisa 56100, Italy

## **S** Supporting Information

**ABSTRACT:** Functional targeted therapy has unfortunately failed to improve the outcome of glioblastoma patients. Success stories evidenced by the use of antibody–drug conjugates in other tumor types are encouraging, but targets specific to glioblastoma and accessible through the bloodstream remain scarce. In the current work, we have identified and characterized novel and accessible proteins using an innovative proteomic approach on six human glioblastomas; the corresponding data have been deposited in the PRIDE database identifier PXD001398. Among several clusters of uniquely expressed proteins, we highlight collagen-VI-alpha-1 (COL6A1) as a highly expressed tumor biomarker with low levels in most normal tissues. Immunohistochemical analysis of glioma samples from 61 patients demonstrated that COL6A1 is a significant and consistent feature of high-grade glioma. Deposits of COL6A1 were evidenced in the perivascular regions of the tumor-associated vasculature and in glioma cells found in pseudopalisade structures. Retrospective analysis of public gene-expression data sets from over 300 glioma patients demonstrated a significant correlation of poor patient outcome and high COL6A1 expression. In a proof-of-concept study, we use chicken chorioallantoic membrane *in vivo* model to show that COL6A1 is a reachable target for IV-injected antibodies. The present data warrant further development of human COL6A1 antibodies for assessing the quantitative biodistribution in the preclinical tumor models.

**KEYWORDS:** biomarkers, angiogenesis, perivascular, targeted therapy, survival



## **I** INTRODUCTION

Glioblastoma is a relatively frequent (20% of all cranial tumors) type of brain tumor with very poor clinical outcome (median survival of 1 year postdiagnosis). Surgery and radiotherapy as well as chemotherapy represent the main axis of treatment, which are essentially palliative in nature. Better understanding of the genetic origins and molecular drivers in glioblastoma<sup>1,2</sup> has opened doors to more tailored, targeted treatments. These consist of small molecules or antibodies, both directed against aberrantly amplified growth factor receptors (and resulting pathways) found on tumor cells (e.g., PDGFR and EGFR) or in tumor-associated vasculature (VEGFR).<sup>3,4</sup> Although the progress made is stunning,<sup>5</sup> the benefits to the patient remain modest despite the enormous financial cost.<sup>6</sup>

Biodistribution studies based on PET (positron emission tomography) imaging show that small molecules do not selectively accumulate in tumors,<sup>7</sup> requiring high, often toxic doses for achieving therapeutic effects. Antibodies have the ability to concentrate in tumors,<sup>8</sup> yet in “naked” format they had only limited success in improving tumor control. A recent trend in targeted therapies is to arm the antibodies with cytotoxic payloads (e.g., cytokines, drugs, photosensitizers).<sup>9,10</sup>

In contrast with the functional-targeted therapy, where protein role in cancer biology is important, cytotoxic, antibody-based targeted therapy requires protein targets that are tumor-specific and systemically accessible. The production of high-affinity human monoclonal antibodies remains a challenging yet a feasible task. Potent cytotoxic drugs are available in large quantities through synthetic routes. However, there is a notable dearth of accessible targets with high expression in neoplastic lesions and absence in normal tissues. In the current study we aimed at identifying novel targetable biomarkers by performing a full proteomic characterization of accessible proteins in human glioblastoma (which we refer to as *accessibilome*). The accessibilome comprises cell-surface and extracellular matrix proteins, which have druggable epitopes *in vivo*. Several established proteomic methods exist for tapping into this group of therapeutically relevant proteins.<sup>11,12</sup> In the present study we use an enrichment technology we previously developed<sup>13–15</sup> to discern proteins that are potentially reachable via systemically injected antibodies. Among several

**Received:** June 28, 2014

**Published:** October 17, 2014

novel targets, we highlight collagens and, in particular, collagen-VI- $\alpha$  1 (COL6A1), a protein barely expressed in normal tissues. Collagens were previously described in glioma;<sup>17</sup> nonetheless, this protein subclass has received little attention in the context of brain tumors until recently.<sup>18–20</sup> Owing to these and similar functional studies, there is growing evidence that collagens serve as a reservoir of secreted growth factors, bind to integrins to induce the formation of intracellular complexes, activate specific tyrosine kinases (e.g., discoidin domain receptors), and provide mechanical support for migration and invasion of cancer cells.<sup>21–23</sup> The current study shows for the first time the feasibility of antibody-based collagen targeting in simplified chicken chorioallantoic membrane (CAM) glioma tumor model *in vivo*. For this purpose, commercially available COL6A1 antibody was first injected in the vasculature and subsequently detected using immunofluorescence in the tumor. The results validate the proteomic findings in human samples, demonstrating that COL6A1 is indeed an accessible target in the CAM model, with potential to serve as molecular anchor for systemically delivered antibodies carrying toxic payloads.

## MATERIALS AND METHODS

### Patients

The material for proteomic study consisted of residual glioblastomas, which were obtained from six patients that underwent surgery. For immunohistochemical validation, paraffin-embedded tissue was used; the material consisted of 38 glioblastomas, 8 astrocytomas GIII, 8 astrocytomas GII, and 7 astrocytomas GI. All human tissue was obtained from the University Hospital, University of Pisa, Italy, and the University Hospital, University of Liege, Belgium. The ethical committee of the University of Liege approved the study.

### Cell Culture and Animal Model

All experimental procedures on animals used in this study were reviewed and approved by the Institutional Animal Care and Use Committee of the University of Liege. The human glioblastoma U87-MG cells (HTB-14) were obtained from the American Type Culture Collection (ATCC; Manassas, VA). The U87 cells were isolated from glioblastoma of 44-year old male caucasian (blood type A, Rh+), they were hypodiploid (44 chromosomes occurring in 48% of cells) with higher ploidy rate of 5.9%. Common genetic features included der(1)t(1;3)(p22;q21), der(16)t(1;16)(p22;p12), del(9)(p13), and only one copy of normal X chromosome. The U87 cells were maintained at 37 °C in Eagle's minimal essential medium supplemented with 10% heat-inactivated fetal calf serum (FCS), 2 mM glutamine, and 1 mM sodium pyruvate (all materials from Invitrogen, Life Technologies, Carlsbad, CA).

Chicken eggs were opened on the third day postfertilization by incising a 2 × 1 cm window in the shell. Eggs were sealed with Durapore tape (3M, Diagem, Belgium) and kept closed at 37 °C and 80% humidity until the 11th day postfertilization. At this time point, CAM was gently lacerated and 5 × 10<sup>6</sup> human U87 glioblastoma cells were deposited in 20  $\mu$ L of culture medium. The eggs were further incubated for an additional 7 days and used on the last day for *in vivo* antibody injections. The injection was performed using CD44 (BBA10, R&D systems, Minneapolis, MN), COL6A1 (LS-B696, LifeSpan Biosciences, Seattle, WA), and IgG (02-6102, Zymed Laboratories, San Francisco, CA) antibodies diluted in saline at a concentration of 0.1 mg/mL (COL6A1 and IgG) and 0.2

mg/mL (CD44). 100  $\mu$ L of antibody solution was injected in the CAM vasculature using a 29G needle on a 1 mL syringe. Sixteen hours postinjection the CAM-containing tumors were collected and frozen in TEK. They were subjected to immunofluorescence analysis as described below. Noninjected CAM tumors were either fixed in formaldehyde and embedded in paraffin or used for accessible biomarker identification.

### Sample Preparation and nanoHPLC–MS/MS Analysis

The *ex vivo* biotinylation procedure was outlined in detail elsewhere.<sup>14</sup> Briefly, fresh tissue samples (of human and CAM origin) were first cut in smaller pieces (~0.125 cm<sup>3</sup>) and immediately soaked into EZ-link Sulfo NHS-SS-biotin (Pierce, Rockford, IL) solution for 15 min, then snap-frozen and pulverized. 1 mg of tissue powder was lysed and subjected to affinity purification of biotinylated proteins using streptavidin. Purified proteins were digested with trypsin (Promega, Madison, WI), and 5  $\mu$ g was analyzed using nanoHPLC–MS/MS approach. The analytical conditions used were described in detail previously.<sup>16</sup> Briefly, the digested proteins were injected on the Bio-X-SCX column (500  $\mu$ m i.d. × 15 mm; Dionex, p/n: 161395). Peptides were fractionated using different concentrations of salt and further separated on the C18 analytical column (Acclaim 75  $\mu$ m × 150 mm, p/n: 162224; Dionex, Sunnyvale, USACA) connected online to Bruker HCTultra ion-trap (Bremen, Germany).

### MS Data Analysis

The acquired MS spectra were processed for peak list generation using the Data Analysis software version 3.4 (Bruker Daltonics, Bremen, Germany), and database search was conducted using the Mascot search engine version 2.2.2 (Matrix Sciences, Boston, MA). Human nonredundant protein database Swissprot (Swiss Institute for Bioinformatics, Basel, Switzerland) version 57.7 was used, and a total of 20 405 entries were searched. The following search parameters were used: enzyme was set for trypsin, one missed cleavage was allowed, mass tolerances of precursor and fragmented ions were set at 0.6 and 0.3, respectively; fixed modification was carbamidomethyl and variable modification was oxidation of methionine. The instrument choice was set to ESI-TRAP. The list of protein hits was further filtered by setting the peptide significance threshold at 0.05 and by requesting at least one bold red peptide per protein hit. As a general rule, only proteins with two or more peptides were further considered. In some occasions, proteins with only one peptide were also included if the peptide match met the above criteria and further manual inspection of MS/MS data confirmed the quality of the hit (signal-to-noise ratio was high, all major peaks were assigned, and no missed cleavages were present). Relative protein abundance (for each sample individually) was determined from the exponentially modified protein abundance index (emPAI)<sup>24</sup> that was calculated directly by Mascot search engine algorithm. The latter considers only peptides with scores above the significance threshold for emPAI calculation. The data were exported as CSV files and visualized using the Multi Experiment Viewer software version 4.8.<sup>25</sup> The potential accessibility of a protein was inferred from Uniprot ([www.uniprot.org](http://www.uniprot.org)) and Human Protein Reference Database (<http://www.hprd.org>) by evaluating information evidencing its cell membrane or extracellular presence. Proteins with unknown cellular localization were also kept in the analysis. The presence of proteins in normal brain tissue was excluded to a far extent by searching for homologue proteins in similar proteomic data

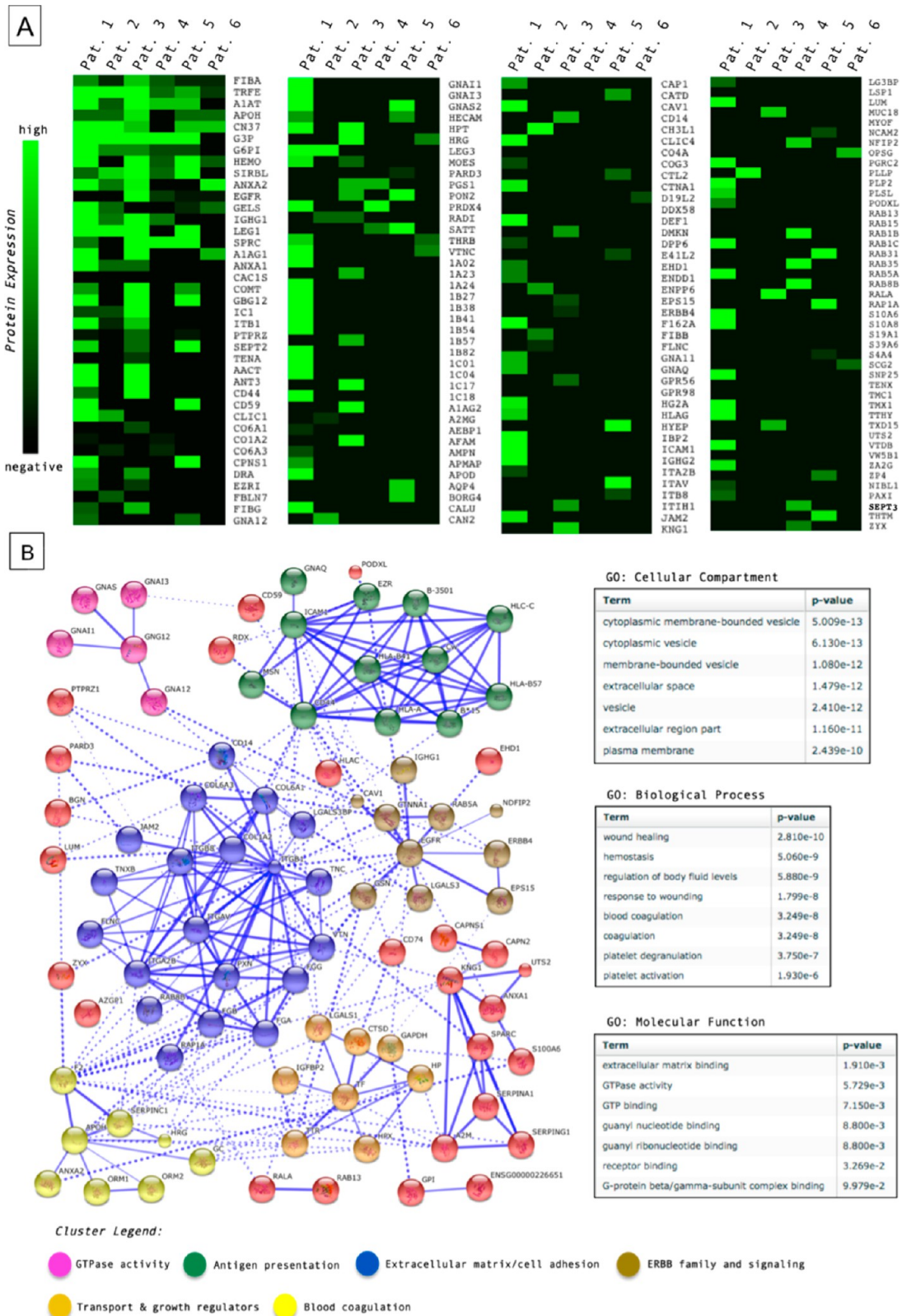


**Figure 1.** Accessibilome of human glioblastoma. (A) Heat-map of 164 accessible proteins identified in proteomic analysis of six patients. None of the proteins were found present in normal mouse brain. The color code corresponds to relative protein quantity, as expressed by emPAI value (see Materials and Methods section). For information concerning the protein score, sequence coverage, number of unique peptides, emPAI value, and presence in CAM, see the Supporting Information, Table S1. (B) Functional clustering using K-means method identifies groups of proteins within the accessibilome of human glioblastoma (according to STRING V9.1 software). Statistically significant enrichment of identified proteins in distinct cellular compartments, biological processes, and molecular functions is displayed with corresponding *p* value.



accrued on mice.<sup>26</sup> The absence of proteins in normal human tissues was confirmed by analyzing publicly deposited DNA microarray ([www.biogps.org](http://www.biogps.org)) and IHC data ([www.proteinatlas.org](http://www.proteinatlas.org)).

### Network Cluster and Statistical Analysis

Modulated proteins were analyzed using the STRING V9.1 software,<sup>27</sup> where protein–protein interactions were interrogated. K-means clustered data were used to spot different functional groups.

Statistical significance for IHC scoring was tested using Mann–Whitney U-Test and SigmaPlot software version 10.0 (Systat, San Jose, CA); the data did not follow the normal distribution (Shapiro–Wilk test). Statistical testing of gene-expression survival data was performed using the Log-rank test (see later).

### Kaplan–Meier Survival Curves

Survival curves and gene expression analysis for COL6A1 were derived in silico utilizing the online tool of the REMBRANDT database<sup>28</sup> (<https://caintegrator.nci.nih.gov/rembrandt/welcome.jsp>).

### Western Blot

Modulated expression of COL1A2, COL6A1, and COL6A3 was verified using Western blot (WB) analysis. Twenty  $\mu\text{g}$  of tissue/cell lysate was loaded and separated on a 7.5% sodium dodecyl sulfate–polyacrylamide gel electrophoresis (SDS-PAGE), transferred to PVDF membranes, and probed with following antibodies: COL1A2 (NBP1-19699, Novus Biologicals, CO), COL6A3 (HPA010080, Sigma-Aldrich, MO), and COL6A1 (HPA019142, Sigma-Aldrich, MO). Protein loading was verified using HSC70 protein expression (K-20, Santa Cruz, Heidelberg, Germany).

### Immunohistochemistry

COL1A2, COL6A1, and COL6A3 were selected for immunohistochemistry-based evaluation. The following antibodies were used: COL1A2 (NBP1-19699, Novus Biologicals, CO), COL6A3 (HPA010080, Sigma-Aldrich, MO), and COL6A1 (HPA019142, Sigma-Aldrich, MO). Additionally, IHC of CD44 expression was performed only on U87-CAM tissue using corresponding anti-CD44 (BBA10, R&D systems, Minneapolis, MN). Five  $\mu\text{m}$  thick paraffin sections were deparaffinized, blocked for endogenous peroxidase activity, and subjected to antigen retrieval in citrate buffer. The sections were blocked accordingly and incubated with the primary antibody at 4 °C overnight. The sections were then washed in PBS and incubated in avidin–biotin complex kit for 30 min. Finally, the tissue sections were stained with 3,3'-diaminobenzidine (DAB; 2 mg DAB and 5  $\mu\text{L}$  of  $\text{H}_2\text{O}_2$  in 5 mL of PBS) and counter-stained in hematoxylin.

The quantification of protein expression was performed only for COL6A1 by two independent evaluators (average values were reported) and according to previously published methodology<sup>29</sup> with minor modifications to the scoring scale. In brief, each IHC slide was assessed for the intensity and extent of positivity. The intensity value 0 denoted an undetectable staining, whereas 1, 2, or 3 denoted low, moderate, and strong immunoreactivity, respectively. The extent of positivity was reported as 1, 2, 3, or 4, referring respectively to  $\leq 25$ , 26–50, 51–75, or 76–100% of the tissue surface showing immunoreactivity. The results were collected in a blind fashion by two observers. Average values obtained from the two scales were then multiplied together, yielding a single value, named score.

### Immunofluorescence

Five  $\mu\text{m}$  thick frozen sections were cut and further fixed in methanol/acetone solution (80:20% v/v) for 10 min. The unspecific reaction was blocked with IgG free BSA solution (1% in PBS) for 1 h. The slides were incubated with Alexa-488 conjugated secondary antibody (Invitrogen) at 4 °C overnight. After extensive washing with PBS and water, the slides were mounted using Vectashield mounting medium with DAPI (cat. no. H-1500; Vector Laboratories, Burlingame, CA) and imaged with fluorescence microscope (A1R, Nikon Instruments, Melville, NY).

## RESULTS

### Accessibilome of Human Glioblastoma Features Distinct Groups of Up-Regulated Proteins

In the current study, we had the opportunity to analyze the potentially accessible proteome of human glioblastoma obtained from six individual patients. However, this cohort is relatively small to allow more general conclusions, especially keeping in mind the broad genetic variability often seen in gliomas. Therefore, we decided to additionally analyze a U87-based CAM model of human glioblastoma, previously shown to veritably depict the situation encountered in humans.<sup>30</sup> CAM tumors were subjected to the same analysis used for human samples. The analysis of six human glioblastomas and three U87 CAM-derived tumors led to the identification of 898 and 633 unique proteins, respectively. In direct comparison of human versus CAM data, 397 proteins were identical, suggesting a proteomic similarity of 63% (in comparison with all proteins identified in CAM model). To exclude proteins, which are highly abundant in normal brain, we have crosschecked the present data with data obtained using normal mouse brain and the same proteomic technique.<sup>26</sup> Mouse brain was selected due to the difficulty to obtain fresh human normal brain samples. This filtering step reduced the number of potentially up-regulated proteins in human glioblastoma to 500 (data shown in Supporting Information). Of these candidates, 32% (164 proteins) were deemed as potentially accessible (according to their annotated subcellular localization) and therefore of value for antibody-based targeting. These proteins are represented in Figure 1A. Clustering analysis using the publicly available STRING software clearly identified several groups of proteins that appear strongly represented in the accessibilome of human glioblastoma (Figure 1B). These are proteins involved in (i) extracellular matrix and adhesion (e.g., tenascin, collagens, integrins, and gallectins), (ii) antigen presentation (e.g., HLA complex), (iii) ERBB signaling (e.g., EGFR, receptor tyrosine-protein kinase erbB-4 [ERBB4]), (iv) GTPase activity (various G-binding proteins), (v) transport and growth regulators (e.g., transthyretin [TTR] and cathepsin D [CTSD]), and (vi) blood coagulation (e.g., beta-2-glycoprotein 1 [APOH]). Of these clusters, the most numerous and statistically significant one (see *p* value for molecular functions) belongs to the group of extracellular matrix and adhesion proteins. Notably, three distinct collagens are reported in this cluster, and we sought to further validate their expression in human glioma and test their suitability to serve as ligands for antibody-based tumor targeting.

### Collagens Are a Constitutive Feature of Human Glioblastoma

To test if collagens, in general, are found in glioblastoma, we have performed a Masson's trichrome staining of 10

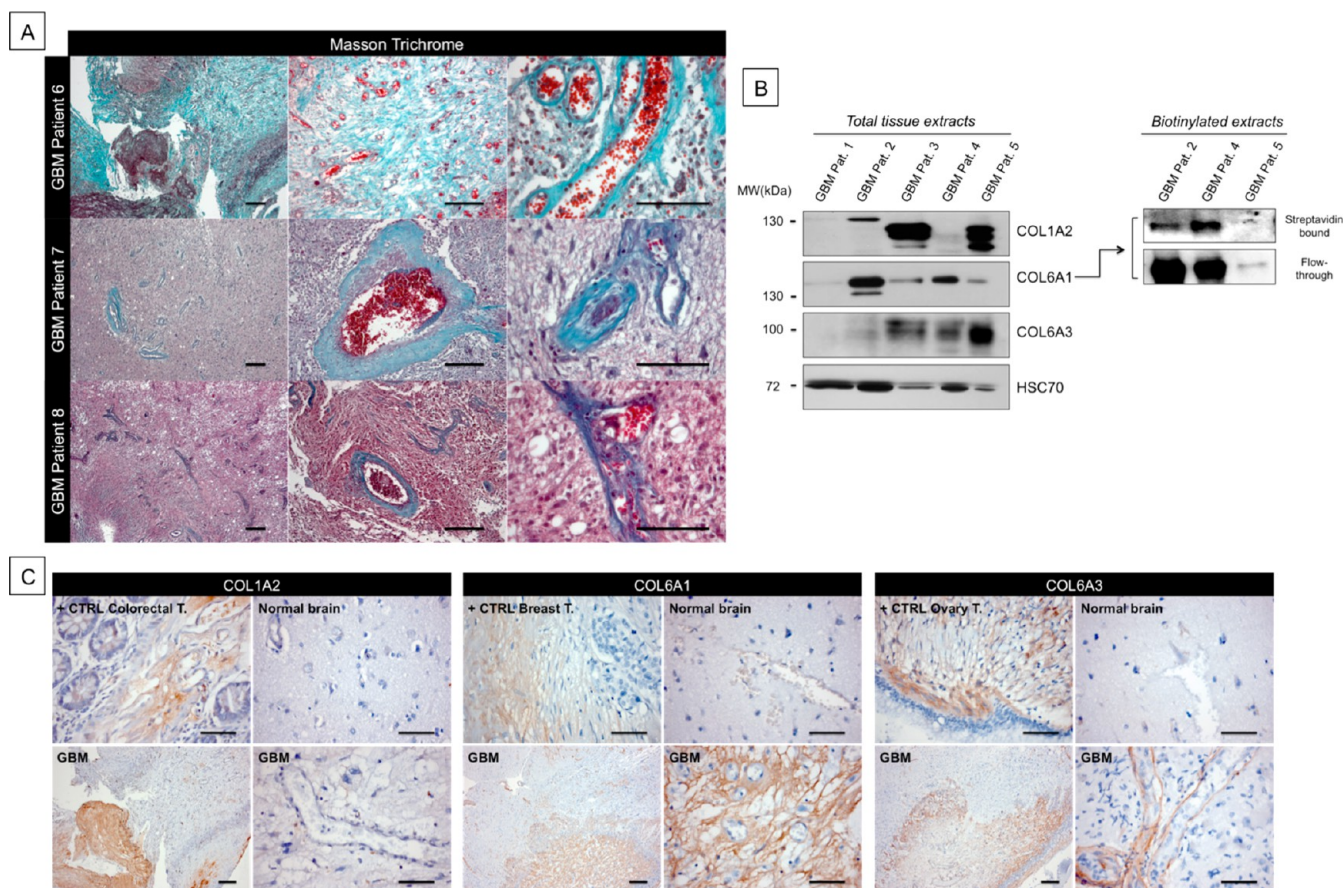


**Figure 2.** Collagens-1-A2, -6-A1, and -6-A3 are consistent features of human glioblastoma. (A) Masson's trichrome staining for qualitative evaluation of collagen presence (blue color) in three cases of human glioblastoma. Three magnifications are displayed: 40, 100, and 400 $\times$ . (B) (left) WB analysis of COL1A2, COL6A1, and COL6A3 protein expression in total tissue extracts of 5 GBM patients and (right) WB of COL6A1 from biotinylated tissue extracts (bound and flow-through fractions) of three GBM patients (same patients were involved in the MS analysis). HSC70 protein is used as loading control. (C) IHC-based qualitative assessment of COL1A2, COL6A1, and COL6A3 protein expression in 10 cases of human glioblastoma (displayed are representative images from a single case); low (40 $\times$ ) and high (100 $\times$ ) magnifications are shown.

glioblastoma cases. As shown using representative cases, collagens are aberrantly expressed in human glioblastoma and are not present in normal adjacent tissue (Figure 2A). These findings are in line with previous studies reporting on collagen expression in glioblastoma.<sup>17–20</sup> Although certain collagens were negative in several patients according to the proteomic analysis (Figure 1A), the expression of COL1A2, COL6A1, and COL6A3 was confirmed using Western blot analysis on the total protein extracts from four out of five glioblastoma patients originally involved in the proteomic study (for patient 6, no additional material was available) (Figure 2B, left). Patient 1 was negative for all collagens tested. Because COL6A1 was identified only in patient 3 in the MS analysis, we also sought to validate the presence of this protein in the accessible fraction of other glioma patients using a targeted approach. For this purpose, biotinylated tissue material originating from patients 2, 4, and 5 (material was available for both MS and WB analysis) was additionally subjected to streptavidin affinity chromatography, followed by WB analysis of bound and flow-through fractions. The results confirm the presence of COL6A1 in the accessible proteome fraction of patients 2 and 4, whereas patient 5 tested negative. The flow-through fraction indicates that the latter patient had very low levels of COL6A1 in the departing material. To expand this limited number of observations and also gain structural insight into the local-

ization of these collagens in high-grade glioma, we have performed IHC analysis using 10 additional cases of glioblastoma (Figure 2C). The analysis confirmed the proteomic and Western blot findings, clearly showing that COL1A2 is expressed in the extracellular matrix and COL6A1 and COL6A3 in perivascular regions. Normal adjacent tissues as well as normal vessels were negative for all three collagens tested. These findings suggested the potential suitability of all three collagens tested to serve as targets for antibody-based targeted therapy approaches.

#### COL6A1 Has Low Expression in a Panel of Normal Human Tissues

Several repositories of human gene expression microarray and tissue microarray data for both malignant and normal tissues are publicly available. In the current study, we have used the data repositories of BioGPS (The Scripps Research Institute, La Jolla, CA) and Protein Atlas (KTH - Royal Institute of Technology, Stockholm, Sweden and the Rudbeck Laboratory, Uppsala University, Uppsala, Sweden) to explore *in silico* the expression patterns of COL1A2, COL6A1, and COL6A3 in normal tissues at gene and protein expression levels (Figure 3). EGFR was selected as a benchmark because two antibody-based targeted therapies are directed toward the EGFR (Panitumumab and Cetuximab) and are currently examined in clinical trials in high-grade glioma patients. As shown in



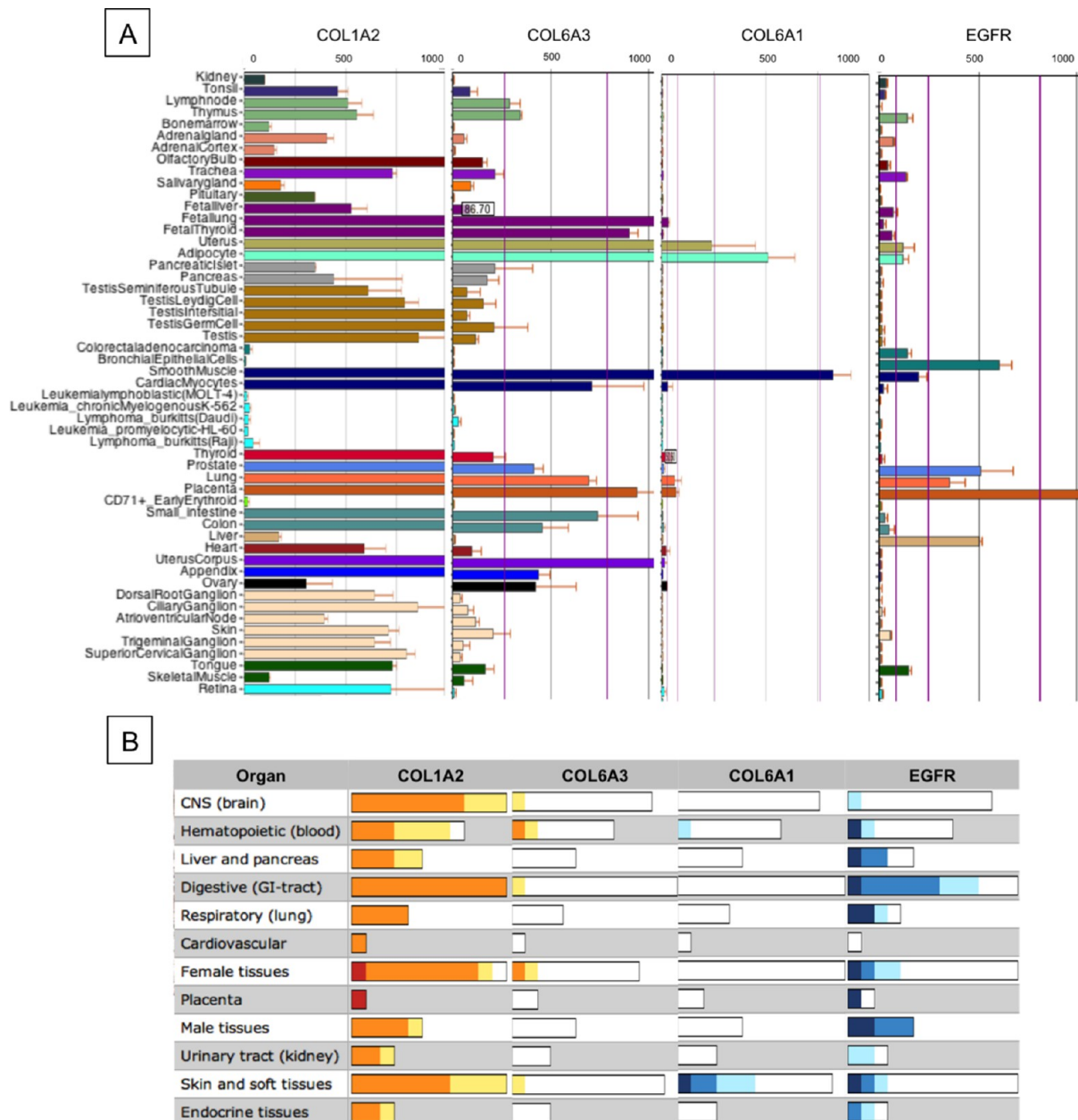


**Figure 3.** COL6A1 is barely expressed in most normal human tissues. (A) In silico evaluation of publicly available DNA gene expression data from Biogps (The Scripps Research Institute, La Jolla, CA) for COL1A2, COL6A1, and COL6A3 expression in normal human tissues and selected human cancers. (B) IHC data on COL1A2, COL6A1, and COL6A3 protein expression obtained in silico from publicly available database Protein Atlas (KTH - Royal Institute of Technology, Stockholm, Sweden and the Rudbeck Laboratory, Uppsala University, Uppsala, Sweden). Scoring of positivity refers only to the cellular component of each organ. Not considered are connective tissue components and extracellular matrix. EGFR expression is used as a benchmark (A,B).

Figure 3A, COL1A2 and COL6A3 are abundantly expressed in various normal tissues at gene expression level. On the contrary, COL6A1 is generally not expressed in normal tissues, except smooth muscle, adipocytes, and uterus. Overall, COL6A1 is positive in fewer normal tissues than EGFR, the latter showing considerable expression in lung, prostate, liver, and bronchial epithelial cells. The observation made at the gene expression level was generally confirmed by the IHC findings (Figure 3B). Several validated antibodies against each protein were tested in a panel of normal tissues by the Protein Atlas consortium. The data show that COL6A1 is not expressed at the protein level in the epithelium of most organs. Higher levels of COL6A1 expression are observable in skin, uterus, and soft

tissues. The latter is probably due to the richness of the respective organs in connective tissue, which appears to be generally positive for COL6A1. However, the intensities of COL6A1 expression appear very different with two distinct antibodies used. COL1A2 and COL6A3 are abundantly expressed in normal tissues. EGFR is surprisingly found significantly expressed in various normal tissues beyond the expected ones according to the gene expression data. The latter underlines the necessity to interrogate proteins in addition to genes because a straightforward correlation is often missing. These data encouraged the further examination of COL6A1 in more cases of human glioma.

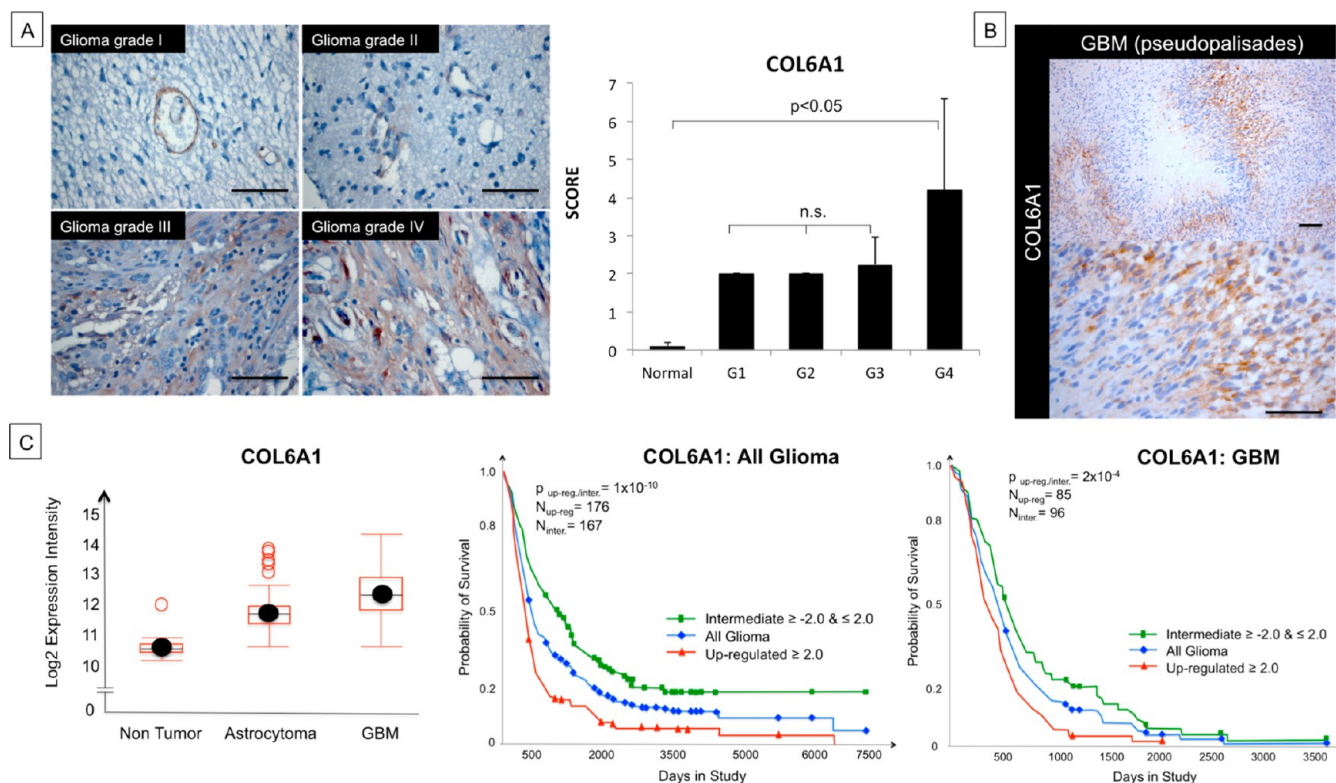


**Figure 4.** COL6A1 is highly expressed in GBM and is a marker of poor clinical outcome. (A) COL6A1 protein expression assessed through IHC in gliomas of different grades (38 glioblastoma, 8 astrocytoma GIII, 8 astrocytoma GII, and 7 astrocytoma GI). Pictures of representative cases for each grade are shown. Semiquantitative evaluation of IHC staining (see Materials and Methods section) showed a significant up-regulation of COL6A1 in grade 4 patients. The scoring for individual patients is outlined in the Supporting Information, Table S2. Error bars indicate standard deviation of means, and  $p$  values have been calculated using Student's  $t$  test (n.s. denotes no significance). (B) COL6A1 is expressed by glioma cells mainly limited to pseudopalisade structures. All IHC images: magnification used (A) 100 $\times$  and (B) 100 $\times$  and 400 $\times$ . (C) Gene expression intensity analysis from publicly deposited data using REMBRANDT web-based tool. From left to right: Box and Whisker log 2 gene-expression intensity plot for nontumoral ( $N = 28$ ), astrocytoma ( $N = 148$ ), and glioblastoma ( $N = 228$ ) samples. Kaplan–Meier survival curves according to expression levels of COL6A1 (intermediate or high) for all glioma or only glioblastoma patients; the respective patient numbers and  $p$  values (log-rank test) are indicated in the graph.

### COL6A1 Is Expressed in All Grades of Human Glioma

To determine if COL6A1 is expressed in all grades of human glioma, we have performed IHC analysis of COL6A1 expression on a limited cohort of grade I to grade IV gliomas (see Materials and Methods section). The data demonstrate (Figure 4A and Supporting Information Table S2) that COL6A1 is indeed expressed at low levels (IHC score 2) in grade I (7/7 patients scored positive), II (8/8 patients scored positive), and III (8/8 patients scored positive); in grade IV, the expression of COL6A1 is significantly higher (IHC score 4) (37/38 patients scored positive). There was no evidence of positive correlation between the different grades and the expression of COL6A1. At the cellular level, the staining was predominantly perivascular. COL6A1 positivity was also evidenced in glioma cells, however, only in those that were found organized in pseudopalisades (Figure 4B). Further analysis of public gene-expression data repository of National Cancer Institute REMBRANDT confirmed the IHC data, highlighting the up-regulation of COL6A1 in glioblastomas with respect to nontumoral and astrocytoma specimens (Figure 4C). Same data were also used to generate gene-expression patient-survival correlations for either all glioma or only glioblastoma cases. The analysis brought forward a statistically significant correlation of high COL6A1 expression with poor outcome (survival) for both patient cohorts (Figure 4C).

### COL6A1 Is Accessible Target in CAM Model of Human Glioblastoma

The specific proteomic approach used in the current study highlights targets that are putatively accessible. Their real accessibility needs, however, to be confirmed using homing antibodies *in vivo*. We have previously demonstrated the usefulness of the U87 CAM model for early preclinical tumor imaging.<sup>31</sup> Along these lines, we have tested in the present study the ability of anti-COL6A1 antibody to reach the tumor in the U87 CAM-based glioblastoma model. As demonstrated in Figure 5A, U87 tumor grown on CAM is highly angiogenic and features functional vasculature (evidenced by the presence of nucleated chicken red blood cells in the vessel lumen). The surrounding CAM is also vascularized, offering IV administration routes for injecting compounds. As a positive control, we have chosen the anti-CD44 antibody because we have identified CD44 as overexpressed in the proteomic analysis (Figure 1), and CD44 antibodies are currently tested for antitumor therapies. In addition, both proteins are confirmed expressed in the U87 CAM model (Figure 5B and proteomic data (Supporting Information)). Sixteen hours post-IV injection of anti-CD44 and anti-COL6A1 antibodies in the CAM, the tumors were excised and prepared for microscopy evaluation. Expectedly, anti-CD44 accumulated in the tumor binding to the cell membrane (Figure 5C). COL6A1 showed



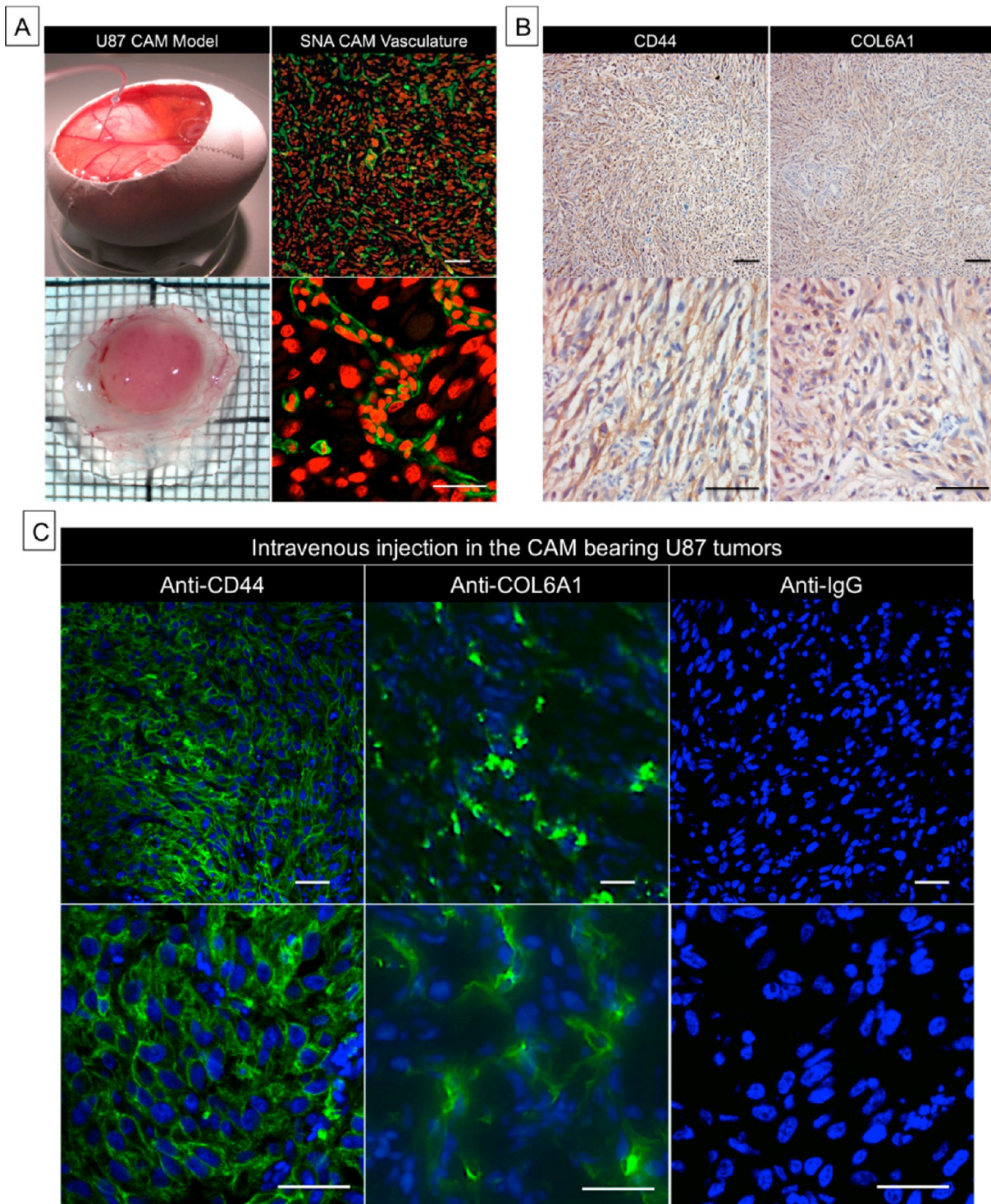


**Figure 5.** COL6A1 is accessible target in U87-based GBM in vivo model. (A) U87 cells implanted on CAM give rise to angiogenic tumors with fully functional vessels. (B) IHC analysis demonstrate that CD44 and COL6A1 are expressed in the U87-CAM glioblastoma model. (C) Homing antibodies against CD44 and COL6A1 injected i.v. are able to reach the U87 tumor and bind to accessible portions of the proteins. Irrelevant antirabbit IgG serves as a negative control. All magnifications: 100X and 400X.

accumulation in the extracellular matrix, specifically in the perivascular regions (Figure 5C). Although COL6A1 is also significantly expressed in the cytosol of U87 cells (Figure 5B), the injected antibody did not internalize, and intracellular pools of COL6A1 remained inaccessible. Injection of the irrelevant antirabbit IgG showed no positivity (binding) in the tumor.

## DISCUSSION

If antibody-based targeted therapies are to become more efficient in glioblastoma patients, it will require more abundant, specific, and accessible biomarkers. Provided the latter are identified, antibody–drug conjugates (which per se do not need to target a protein function) are a good way forward to escalate the dose selectively in the tumor. In the current study,



we had the unique opportunity to characterize the accessible proteome of human glioblastoma. The clustering analysis of modulated proteins clearly identified a set of collagens that were uniquely found in the tumor. To our knowledge, the present data associate for the first time collagens in high-grade glioma with accessibility as an important feature for therapeutic application. The identification of COL6A1 is particularly relevant because this protein has low expression in most normal human tissues, qualifying it as a promising target for antibody-based tumor therapy. The present data show that COL6A1 expression in glioblastomas is to a great extent limited to the perivascular region. Apart from this, COL6A1 is also found in glioma cells, however, only in those that are organized in pseudopalisades. Glioma cells forming pseudopalisades are typical of high-grade gliomas, increasingly found around necrotic hotspots.<sup>32</sup> They are in a state of organized migration away from necrotic areas, featuring increased expression of pro-angiogenic factors, for example, VEGF, HIF1/2, and MMPs.<sup>33</sup> The current findings indicate that COL6A1 may be expressed by this particular class of glioma cells that master the evasion of hostile conditions and are probably at the core of glioma's ability to adapt and survive all therapies available today. In support of this is the present correlation analysis of patient-survival and COL6A1 gene-expression, demonstrating a significant positive correlation between high COL6A1 levels and poor outcome of glioma patients in general and glioblastoma in specific. The notion that COL6A1 function may correlate with angiogenesis is strengthened by the recent findings of Kojima et al.<sup>34</sup> The authors detected a marked mRNA overexpression of COL6A1 in rat brain cortex following hypoxic-ischemic brain injury. This study indicates that COL6A1 expression may also be induced in normal brains after injury that is potentially related to reduced blood flow (e.g., stroke).

Accessibility is an important feature of any target that may be exploited for cytotoxic antibody-based targeted therapies. Accessibility refers to the process where a homing antibody injected in the vasculature reaches and binds to the target. To test if COL6A1 is a reachable target, we have employed a simplified glioblastoma model, which is based on U87 cells growing on CAM. This model does not recapitulate all of the functional features of glioblastoma; however, the antibody-based toxic targeting does not rely on function but rather on the physical presence or absence of the target. We therefore chose U87 model because it is highly angiogenic and the cells express COL6A1 protein. The data show that, systemically injected, COL6A1 antibodies can successfully reach the tumor in vivo. Future development of COL6A1 antibody-based therapy will certainly profit from the tumor vessel proximity of the COL6A1 target, which is also evident in the CAM. Conjugation of beta-emitters, like <sup>188</sup>Re, to the COL6A1 antibody would then allow irradiation depths of several millimeters, reducing the importance of the antibody ability to diffuse inside the tumor. However, one major limitation of the present CAM model is that it does not account for the effect of the blood–brain barrier (BBB), which would represent an effective hurdle to antibody leaving the brain vasculature. In glioblastoma, BBB is usually compromised, which can favor the antibody delivery, but this has to be put in balance with high interstitial pressures resulting from dysfunctional BBB. The present results therefore warrant future quantitative biodistribution studies in murine glioma models, possibly in combination with vascular remodeling agents (e.g., Bevacizu-

mab).<sup>35,36</sup> In the current proof-of-principle we use commercial polyclonal antibody of research-grade quality. The preclinical experiments will be meaningful only if new COL6A1 high-affinity human antibodies are developed prior to further tests in murine models. These antibodies should ideally be considered in different formats (e.g., full IgG and small immunoproteins) to optimize the pharmacokinetics and drug delivery.

## ■ ASSOCIATED CONTENT

### 📄 Supporting Information

Table S1. Accessible proteins in human glioblastoma. Table of proteins identified as potentially accessible (see Figure 1) along with relevant information on Swissprot database search results. Following information is provided (from left to right): accession name, full protein name, frequency of identification in 6 human patients studied, protein presence in the CAM model (X denotes presence), protein score as indicated by the Mascot database search, number of matched peptides (unique peptides, equal/above the significance threshold of 0.05), sequence coverage in % and empAI values as calculated by the Mascot search engine. Table S2. COL6A1 quantification in a collection of human gliomas and normal adjacent human brain. Quantification of COL6A1 expression was conducted by evaluating the positivity (P) and extent (E) of the IHC staining (score =  $P \times E$ ); the procedure is detailed in the Materials and Methods section. This material is available free of charge via the Internet at <http://pubs.acs.org>. The mass spectrometry proteomics data have been deposited to the ProteomeXchange Consortium<sup>37</sup> via the PRIDE partner repository with the data set identifier PXD001398.

## ■ AUTHOR INFORMATION

### Corresponding Author

\*E-mail: [a.turtoi@ulg.ac.be](mailto:a.turtoi@ulg.ac.be).

### Author Contributions

#A.T. and A.B. contributed equally.

### Notes

The authors declare no competing financial interest.

## ■ ACKNOWLEDGMENTS

This work was supported by a grant from the Research Concerted Action (IDEA project) of the University of Liège (ULG), Belgium, from the National Fund for Scientific Research (FNRS, Belgium) and TELEVIE, as well as from the Centre Anti-Cancéreux of the ULG and the CEE (FP7 network: ADAMANT-Antibody Derivatives As Molecular Agents for Neoplastic Targeting (HEALTH-F2-2007-201342)). A.T. is a Research Fellow of FNRS and A.B. is Doctoral Fellow of FNRS/Televie. We acknowledge GIGA-Proteomics platform, GIGA-Imaging platform, ULG Biobank, Dr. Davide Musmeci, and Brunella Costanza for experimental support. We are particularly thankful to Pascale Heneaux and Evgenia Turtoi for the IHC experiments.

## ■ REFERENCES

- (1) Huse, J. T.; Holland, E. C. Targeting brain cancer: advances in the molecular pathology of malignant glioma and medulloblastoma. *Nat. Rev. Cancer*. **2010**, *10* (5), 319–331.
- (2) Huse, J. T.; Holland, E.; DeAngelis, L. M. Glioblastoma: molecular analysis and clinical implications. *Annu. Rev. Med.* **2013**, *64*, 59–70.

- (3) Tanaka, S.; Louis, D. N.; Curry, W. T.; Batchelor, T. T.; Dietrich, J. Diagnostic and therapeutic avenues for glioblastoma: no longer a dead end? *Nat. Rev. Clin. Oncol.* **2013**, *10* (1), 14–26.
- (4) Polivka, J., Jr.; Polivka, J.; Rohan, V.; Topolcan, O.; Ferda, J. New molecularly targeted therapies for glioblastoma multiforme. *Anticancer Res.* **2012**, *32* (7), 2935–2946.
- (5) Strebhardt, K.; Ullrich, A. Paul Ehrlich's magic bullet concept: 100 years of progress. *Nat. Rev. Cancer.* **2008**, *8* (6), 473–480.
- (6) Keefe, D. M.; Bateman, E. H. Tumor control versus adverse events with targeted anticancer therapies. *Nat. Rev. Clin. Oncol.* **2011**, *9* (2), 98–109.
- (7) van der Veldt, A. A.; Smit, E. F.; Lammertsma, A. A. Positron Emission Tomography as a Method for Measuring Drug Delivery to Tumors in vivo: The Example of [(11)C]docetaxel. *Front. Oncol.* **2013**, *3*, 208.
- (8) Tabrizi, M.; Bornstein, G. G.; Suria, H. Biodistribution mechanisms of therapeutic monoclonal antibodies in health and disease. *AAPS J.* **2010**, *12* (1), 33–43.
- (9) Pasche, N.; Neri, D. Immunocytokines: a novel class of potent armed antibodies. *Drug Discovery Today.* **2012**, *17* (11–12), 583–590.
- (10) Senter, P. D.; Sievers, E. L. The discovery and development of brentuximab vedotin for use in relapsed Hodgkin lymphoma and systemic anaplastic large cell lymphoma. *Nat. Biotechnol.* **2012**, *30* (7), 631–637.
- (11) He, J.; Liu, Y.; Lubman, D. M. Targeting glioblastoma stem cells: cell surface markers. *Curr. Med. Chem.* **2012**, *19* (35), 6050–6055.
- (12) Liu, Y.; He, J.; Lubman, D. M. Characterization of membrane-associated glycoproteins using lectin affinity chromatography and mass spectrometry. *Methods Mol. Biol.* **2013**, *951*, 69–77.
- (13) Castronovo, V.; Kischel, P.; Guillonnet, F.; de Leval, L.; Defécherieux, T.; De Pauw, E.; Neri, D.; Waltregny, D. Identification of specific reachable molecular targets in human breast cancer using a versatile ex vivo proteomic method. *Proteomics.* **2007**, *7* (8), 1188–1196.
- (14) Turtoi, A.; Dumont, B.; Greffe, Y.; Blomme, A.; Mazzucchelli, G.; Delvenne, P.; Mutijima, E. N.; Lifrange, E.; De Pauw, E.; Castronovo, V. Novel comprehensive approach for accessible biomarker identification and absolute quantification from precious human tissues. *J. Proteome Res.* **2011**, *10* (7), 3160–3182.
- (15) Turtoi, A.; De Pauw, E.; Castronovo, V. Innovative proteomics for the discovery of systemically accessible cancer biomarkers suitable for imaging and targeted therapies. *Am. J. Pathol.* **2011**, *178* (1), 12–18.
- (16) Turtoi, A.; Musmeci, D.; Wang, Y.; Dumont, B.; Somja, J.; Bevilacqua, G.; De Pauw, E.; Delvenne, P.; Castronovo, V. Identification of novel accessible proteins bearing diagnostic and therapeutic potential in human pancreatic ductal adenocarcinoma. *J. Proteome Res.* **2011**, *10* (9), 4302–4313.
- (17) Paulus, W.; Roggendorf, W.; Schuppan, D. Immunohistochemical investigation of collagen subtypes in human glioblastomas. *Virchows Arch. A: Pathol. Anat. Histopathol.* **1988**, *413* (4), 325–332.
- (18) Mammoto, T.; Jiang, A.; Jiang, E.; Panigrahy, D.; Kieran, M. W.; Mammoto, A. Role of Collagen Matrix in Tumor Angiogenesis and Glioblastoma Multiforme Progression. *Am. J. Pathol.* **2013**, *183* (4), 1293–1305.
- (19) Payne, L. S.; Huang, P. The pathobiology of collagens in glioma. *Mol. Cancer Res.* **2013**, *1* (10), 1129–1140.
- (20) Fujita, A.; Sato, J. R.; Festa, F.; Gomes, L. R.; Oba-Shinjo, S. M.; Marie, S. K.; Ferreira, C. E.; Sogayar, M. C. Identification of COL6A1 as a differentially expressed gene in human astrocytomas. *GMR, Genet. Mol. Res.* **2008**, *7* (2), 371–378.
- (21) Sweeney, S. M.; Orgel, J. P.; Fertala, A.; McAuliffe, J. D.; Turner, K. R.; Di Lullo, G. A.; Chen, S.; Antipova, O.; Perumal, S.; Ala-Kokko, L.; Forlino, A.; Cabral, W. A.; Barnes, A. M.; Marini, J. C.; San Antonio, J. D. Candidate cell and matrix interaction domains on the collagen fibril, the predominant protein of vertebrates. *J. Biol. Chem.* **2008**, *283* (30), 21187–21197.
- (22) Leitinger, B. Transmembrane collagen receptors. *Annu. Rev. Cell Dev. Biol.* **2011**, *27*, 265–290.
- (23) Fu, H. L.; Valiathan, R. R.; Arkwright, R.; Sohail, A.; Mihai, C.; Kumarasiri, M.; Mahasenan, K. V.; Mobashery, S.; Huang, P.; Agarwal, G.; Fridman, R. Discoidin domain receptors: unique receptor tyrosine kinases in collagen-mediated signaling. *J. Biol. Chem.* **2013**, *288* (11), 7430–7437.
- (24) Ishihama, Y.; Oda, Y.; Tabata, T.; Sato, T.; Nagasu, T.; Rappsilber, J.; Mann, M. Exponentially modified protein abundance index (emPAI) for estimation of absolute protein amount in proteomics by the number of sequenced peptides per protein. *Mol. Cell. Proteomics* **2008**, *4* (9), 1265–1272.
- (25) Saeed, A. I.; Bhagabati, N. K.; Braisted, J. C.; Liang, W.; Sharov, V.; Howe, E. A.; Li, J.; Thiagarajan, M.; White, J. A.; Quackenbush, J. TM4 microarray software suite. *Methods Enzymol.* **2006**, *411*, 134–193.
- (26) Turtoi, A.; Musmeci, D.; Naccarato, A. G.; Scatena, C.; Ortenzi, V.; Kiss, R.; Murtas, D.; Patsos, G.; Mazzucchelli, G.; De Pauw, E.; Bevilacqua, G.; Castronovo, V. Sparc-like protein 1 is a new marker of human glioma progression. *J. Proteome Res.* **2012**, *11* (10), 5011–5021.
- (27) Franceschini, A.; Szklarczyk, D.; Frankild, S.; Kuhn, M.; Simonovic, M.; Roth, A.; Lin, J.; Minguez, P.; Bork, P.; von Mering, C.; Jensen, L. J. STRING v9.1: protein-protein interaction networks, with increased coverage and integration. *Nucleic Acids Res.* **2013**, No. Database issue, D808–D815.
- (28) Madhavan, S.; Zenklusen, J. C.; Kotliarov, Y.; Sahni, H.; Fine, H. A.; Buetow, K. Rembrandt: helping personalized medicine become a reality through integrative translational research. *Mol. Cancer Res.* **2009**, *7* (2), 157–167.
- (29) Waltregny, D.; Bellahcène, A.; Van Riet, I.; Fisher, L. W.; Young, M.; Fernandez, P.; Dewé, W.; de Leval, J.; Castronovo, V. Prognostic value of bone sialoprotein expression in clinically localized human prostate cancer. *J. Natl. Cancer Inst.* **1998**, *90* (13), 1000–1008.
- (30) Javerzat, S.; Franco, M.; Herbert, J.; Platonova, N.; Peille, A. L.; Pantescio, V.; De Vos, J.; Assou, S.; Bicknell, R.; Bikfalvi, A.; Hagedorn, M. Correlating global gene regulation to angiogenesis in the developing chick extra-embryonic vascular system. *PLoS One* **2009**, *4* (11), e7856.
- (31) Warnock, G.; Turtoi, A.; Blomme, A.; Bretin, F.; Bahri, M. A.; Lemaire, C.; Libert, L. C.; Seret, A. E.; Luxen, A.; Castronovo, V.; Plenevaux, A. R. In vivo PET/CT in a human glioblastoma chicken chorioallantoic membrane model: a new tool for oncology and radiotracer development. *J. Nucl. Med.* **2013**, *54* (10), 1782–1788.
- (32) Wippold, F. J., 2nd; Lämmle, M.; Anatelli, F.; Lennerz, J.; Perry, A. Neuropathology for the neuroradiologist: palisades and pseudopalisades. *Am. J. Neuroradiol.* **2006**, *27* (10), 2037–2041.
- (33) Brat, D. J.; Castellano-Sanchez, A. A.; Hunter, S. B.; Pecot, M.; Cohen, C.; Hammond, E. H.; Devi, S. N.; Kaur, B.; Van Meir, E. G. Pseudopalisades in glioblastoma are hypoxic, express extracellular matrix proteases, and are formed by an actively migrating cell population. *Cancer Res.* **2004**, *64* (3), 920–927.
- (34) Kojima, T.; Ueda, Y.; Sato, A.; Sameshima, H.; Ikenoue, T. Comprehensive gene expression analysis of cerebral cortices from mature rats after neonatal hypoxic-ischemic brain injury. *J. Mol. Neurosci.* **2013**, *49* (2), 320–327.
- (35) Jain, R. K.; di Tomaso, E.; Duda, D. G.; Loeffler, J. S.; Sorensen, A. G.; Batchelor, T. T. Angiogenesis in brain tumours. *Nat. Rev. Neurosci.* **2007**, *8* (8), 610–622.
- (36) Jain, R. K. Normalization of tumor vasculature: an emerging concept in antiangiogenic therapy. *Science* **2005**, *307* (5706), 58–62.
- (37) Vizcaino, J. A.; Deutsch, E. W.; Wang, R.; Csordas, A.; Reisinger, F.; Ríos, D.; Dianos, J. A.; Sun, Z.; Farrar, T.; Bandeira, N.; Binz, P. A.; Xenarios, I.; Eisenacher, M.; Mayer, G.; Gatto, L.; Campos, A.; Chalkley, R. J.; Kraus, H. J.; Albar, J. P.; Martinez-Bartolomé, S.; Apweiler, R.; Omenn, G. S.; Martens, L.; Jones, A. R.; Hermjakob, H. ProteomeXchange provides globally co-ordinated proteomics data submission and dissemination. *Nat. Biotechnol.* **2014**, *30* (3), 223–226.